

Snow-Level Estimates Using Operational Polarimetric Weather Radar Measurements

SERGEY Y. MATROSOV

Cooperative Institute for Research in Environmental Sciences, University of Colorado Boulder, and NOAA/Earth System Research Laboratory, Boulder, Colorado

ROBERT CIFELLI AND ALLEN WHITE

NOAA/Earth System Research Laboratory, Boulder, Colorado

TIMOTHY COLEMAN

Cooperative Institute for Research in Environmental Sciences, University of Colorado Boulder, and NOAA/Earth System Research Laboratory, Boulder, Colorado

(Manuscript received 3 October 2016, in final form 28 December 2016)

ABSTRACT

Scanning polarimetric measurements from the operational Weather Surveillance Radar-1988 Doppler (WSR-88D) systems are evaluated for the retrievals of snow-level (SL) heights, which are located below the 0°C isotherm and represent the altitude within the melting layer (ML) where snow changes to rain. The evaluations are conducted by intercomparisons of the SL estimates obtained from the Beale Air Force Base WSR-88D unit (KBBX) during a wet season 6-month period (from October 2012 to March 2013) and robust SL height measurements h_{SL} from a high-resolution vertically pointing Doppler snow-level profiler deployed near Oroville, California. It is shown that a mean value height measurement h_{L3} between the estimates of the ML top and bottom, which can be derived from the WSR-88D level-III (L3) ML products, provides relatively unbiased estimates of SL heights with a standard deviation of about 165 m. There is little azimuthal variability in derived values of h_{L3} , which is, in part, due to the use of higher radar beam tilts and azimuthal smoothing of the level-III ML products. Height estimates h_{rho} based on detection of the ML minima of the copolar cross-correlation coefficient ρ_{hv} calculated from the WSR-88D level-II products are slightly better correlated with profiler-derived SL heights, though they are biased low by about 113 m with respect to h_{SL} . If this bias is accounted for, the standard deviation of the ρ_{hv} minima-based SL estimates is generally less than 100 m. Overall, the results of this study indicate that, at least for closer radar ranges (up to ~13–15 km), the operational radar polarimetric data can provide snow-level estimates with a quality similar to those from the dedicated snow-level radar profilers.

1. Introduction

The melting layer (ML) in the atmosphere represents a transition region where precipitating ice hydrometeors (e.g., snowflakes) melt and turn into raindrops. In weather radar observations, the ML is usually manifested as a band of enhanced radar reflectivity, so it is often referred to as the radar bright band (BB), which is a common feature of stratiform precipitation. The ML top coincides with the freezing level (FL), which corresponds to the 0°C isotherm and in some applications is

called the melting level. Melting-layer thicknesses can vary from a few hundred meters to about 0.6 km (e.g., Matrosov 2008). Precipitating hydrometeors are composed of ice at the ML top and raindrops at the ML bottom.

One parameter used by National Weather Service (NWS) forecasters is the snow level (SL), which is an altitude where the precipitation type transitions from mostly snow to mostly rain (e.g., White et al. 2010). Unlike the ML, which represents the height interval between the ML top and the ML bottom, the SL refers to a single altitude above the ground. The snow level is essential to many practical applications, such as hydrometeorological forecasts, since, upon reaching the

Corresponding author e-mail: Sergey Y. Matrosov, sergey.matrosov@noaa.gov

surface, it determines where approximately half of precipitation flux contributes to snow accumulation and the other half to water runoff, which typically happens at surface air temperatures of around $+1.5^{\circ}\text{C}$ (Lundquist et al. 2008). The SL is an especially important forecast quantity in mountainous terrain regions since changes in the height of the SL can determine whether a precipitating event is likely to produce mostly rain in the watershed, which may lead to flash flooding, or whether the precipitation will mostly fall as snow and may not have an immediate effect on streamflow (White et al. 2010).

Because the snow level is an important parameter for the weather forecast community, the National Oceanic and Atmospheric Administration (NOAA)/Earth System Research Laboratory (ESRL)/Physical Sciences Division (PSD) and the Cooperative Institute for Research in Environmental Sciences (CIRES) at the University of Colorado Boulder developed and deployed a network of low-cost, high-resolution (~ 40 m), vertically pointing snow-level radar profilers, which utilize the frequency modulated–continuous wave (FM–CW) technology (White et al. 2013). These radars and also some other vertically pointing PSD radars (e.g., wind profilers) are used for SL operational retrievals. The ESRL SL retrieval algorithm (White et al. 2002) uses the combination of echo power and vertical Doppler velocity measurements to infer snow-level estimates as an altitude of maximum reflectivity in the BB (i.e., in the ML), which is on average about 0.2 km lower than the FL height (Lundquist et al. 2008).

The vertically pointing, radar-derived SL estimates were validated using closely collocated radiosonde soundings and were found to be robust (White et al. 2002). These estimates are routinely available online in near–real time from a NOAA website (<http://www.esrl.noaa.gov/psd/data/obs/>). An example of the SL estimates at one of the ESRL PSD observational sites located near Oroville (OVL), California, is shown in Fig. 1, where hourly mean SL heights were retrieved for an extended period of observed precipitation (~ 0900 – 2200 UTC 23 December 2012). It can be seen from this figure that SL heights can change rather significantly over relatively short time intervals, while near-surface temperatures change very little. This indicates the importance of monitoring SL heights in near–real time.

While measurements from vertically pointing radars provide reliable high-temporal- and high-vertical-resolution estimates of snow levels, their major limitation is that they are point measurements that are confined to the locations where such radars are deployed. Since the melting layer also produces distinct signatures in scanning radar measurements, these measurements can

be used for inferring area estimates of SL heights. The BB reflectivity enhancements are often observed in measurements taken in stratiform precipitation at different radar beam tilts. The addition of polarimetric variables significantly enhances scanning radar capabilities for estimating ML boundaries. Polarimetric-radar-based techniques have been developed and used for automatic designation of the melting layer (e.g., Brandes and Ikeda 2004; Matrosov et al. 2007; Giangrande et al. 2008; Boodoo et al. 2010; Keränen et al. 2015; Wolfensberger et al. 2016). Some of these techniques are applied for operational radar observations and corresponding data products, such as melting-layer Next Generation Weather Radar (NEXRAD) level-III products, which are now available to users (<https://www.ncdc.noaa.gov/data-access/radar-data/nexrad-products>).

The objective of this study is to evaluate polarimetric-radar-based ML detection techniques and corresponding data products for the operational use in snow-level retrievals. This evaluation is performed using statistical intercomparisons of the ML characteristics inferred from scanning radar observations and robust SL retrieval results from vertically pointing snow-level radar measurements.

2. Measurement sites and periods of observations

The NEXRAD network of S-band (~ 3 GHz) Weather Surveillance Radar-1988 Doppler (WSR-88D) units, which were recently polarimetrically upgraded, covers most of the continental United States (CONUS). NOAA vertically pointing snow-level radars operate primarily in areas of the western United States. Quantitative intercomparisons of closely collocated in space and time retrievals of melting-layer and snow-level characteristics from WSR-88D and NOAA snow-level radar measurements provide an opportunity for an evaluation/verification of the NEXRAD ML products. In this study, measurements/products from the OVL snow-level radar profiler and the Beale Air Force Base WSR-88D unit (KBBX) were used for detailed evaluations.

Figure 2 shows the locations of the KBBX (39.4956°N , 121.6316°W , 64 m MSL) and OVL (39.5318°N , 121.4876°W , 114 m MSL) radars in the western foothills of the Sierra Nevada near Lake Oroville, which is the second-largest water reservoir in California. The OVL site is located at a distance of about 13 km from the KBBX radar location in the azimuthal direction of approximately 72° . Such a close relative position of the two radars allows for a close collocation of the ML and SL characteristics. Intercomparisons are conducted under conditions of high variability in ML/SL heights,

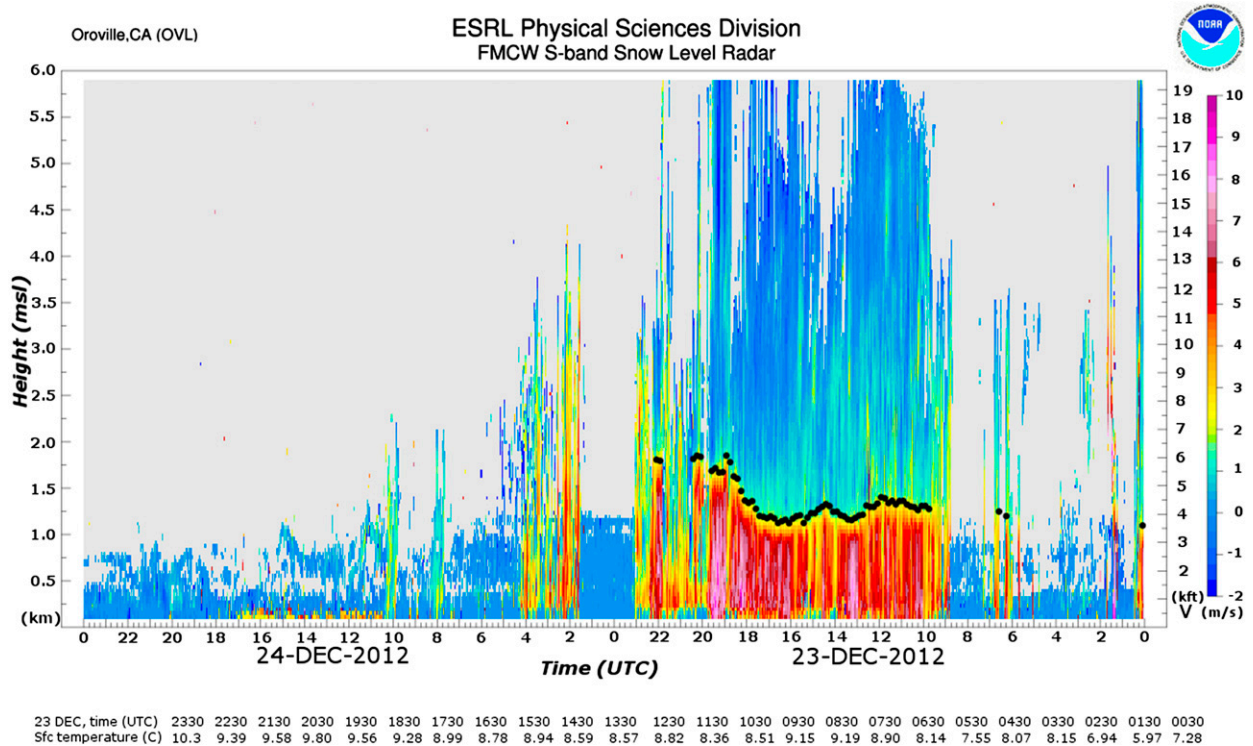


FIG. 1. An example of NOAA/ESRL/PSD-retrieved SL heights (MSL) at the OVL site for 23 and 24 Dec 2012 (note that the time increases from right to left on the x axis). (top) Time–height cross sections of observed vertical Doppler velocity V and corresponding hourly mean SL heights (black dots), and (bottom) a table showing hourly mean 2-m air temperatures for 23 Dec 2012.

which is observed during the cool season near the OVL location.

Since most of the precipitation in central California occurs during the October–March cool season period (e.g., ~80% of total annual precipitation at Oroville is observed during this period and practically all precipitation reaches the surface as rain), the data collected during this season are deemed as an appropriate representation of precipitation characteristics for the purpose of this study. The cool season period from October 2012 through March 2013, which was the wettest since the polarimetric upgrade of the KBBX radar, was chosen here for intercomparisons of ML/SL retrievals.

A total of 26 significant precipitation events, which exhibited consistent SL retrievals by the OVL snow-level radar measurements during KBBX operations, were observed from 1 October 2012 to 31 March 2013. Durations of these events varied from about 2 to 20 h. These precipitation events were observed under different temperature conditions, resulting in the SL heights ranging from approximately 0.6 to more than 2.5 km MSL. The WSR-88D KBBX and OVL radar data collected during these events provided the dataset analyzed in this study.

3. Polarimetric radar retrieval approaches

In addition to enhancements in observed equivalent radar reflectivity factor Z_e (hereafter just reflectivity), the ML provides distinct patterns in measured polarimetric variables. For traditional horizontal–vertical (h–v) polarization states, these patterns include a general enhancement in the differential reflectivity factor Z_{DR} , which is defined as the logarithmic difference between reflectivities on the horizontal and vertical polarizations; an increase in the linear depolarization ratio (LDR), which represents the logarithmic difference of reflectivities in the cross- and copolarized receiving channels for a single polarization transmission; and a sharp decrease in the copolar correlation coefficient ρ_{hv} , which is defined as (e.g., [Bringi and Chandrasekar 2001](#))

$$\rho_{hv} = |\langle V_h V_v^* \rangle| / (\langle |V_h|^2 \rangle \langle |V_v|^2 \rangle)^{0.5}, \quad (1)$$

where V_h and V_v are the copolar complex voltages of the radar returns on the horizontal and vertical polarizations, respectively, the asterisk is the complex conjugation sign, and the angle brackets denote sample averaging.

Often the operational weather radars (e.g., the WSR-88D network) conduct measurements in the

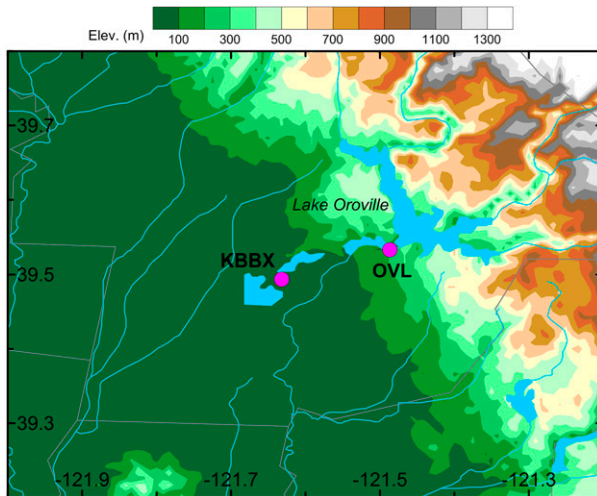


FIG. 2. A map showing the locations of the NOAA snow-level OVL radar and the KBBX WSR-88D unit.

simultaneous (h and v polarizations) transmission–simultaneous (h and v polarizations) receiving (STSR) mode, so LDR measurements are not available and the polarimetric-radar-based ML designation procedures are based on Z_e , Z_{DR} , and ρ_{hv} measurements. The copolar correlation coefficient measurements are primarily sensitive to a degree of scatterer nonuniformity, which is high in the melting layer; are generally a robust ML indicator; and are often distinct even in situations when ML reflectivity enhancement signatures are not very pronounced (e.g., Matrosov et al. 2007).

The correlation coefficient measurements are independent of the radar absolute calibration errors, and ρ_{hv} minima in the ML are usually sharper and less noisy (given a good signal-to-noise ratio) than the reflectivity and differential reflectivity maxima (e.g., Matrosov et al. 2007). The ρ_{hv} minima, however, are typically located lower within the ML than reflectivity maxima (e.g., Giangrande et al. 2008), which can be explained by the fact that, unlike ρ_{hv} , Z_e depends on hydrometeor concentrations, which are larger at higher altitudes within the ML because of the mass flux divergence associated with the general increase of hydrometeor fall velocities as the melting process progresses.

a. Copolar correlation coefficient–based estimates of snow levels

Since the relative sharpness of ρ_{hv} measurements makes it convenient for identifying a single level within a melting layer, it is instructive to statistically evaluate the displacement between WSR-88D-derived copolar cross-correlation coefficient minimum heights $h_{r\theta}$ and NOAA profiler–based snow-level radar SL heights h_{SL} , even though the ρ_{hv} minima are expected to be generally

lower than the SL (i.e., on average, $h_{SL} > h_{r\theta}$). In this study, ρ_{hv} minima were identified along the KBBX radar slant beam measurements in the direction of the OVL observational site (i.e., in the 72° azimuthal direction). NEXRAD level-II products were used for this purpose. The slant radar ranges where the copolar correlation coefficient values were smaller than a 0.92 threshold and where they reached a minimum in the atmospheric column approximately above the OVL site were identified. The ρ_{hv} minima locations were required to be generally consistent with enhanced Z_e and Z_{DR} values ($Z_e > 28$ dBZ, and $Z_{DR} > 1$ dB, correspondingly). These slant ranges were then recalculated to the ρ_{hv} minima heights above mean sea level using approaches for the spherical Earth atmosphere and mean refractive index (Doviak and Zrníc 1993, section 2.2.3). The Earth sphericity and refraction effects, however, are generally negligible for radar ranges corresponding to the KBBX–OVL distance. The ρ_{hv} minima heights were sought within a window interval (typically ± 1.5 km) around the climatological 0°C isotherm height or around a model forecast 0°C isotherm height (if available).

Depending on ML heights, the slant KBBX radar ranges reach the ML over the OVL site for different radar beam tilts. Therefore, different radar tilts were used to retrieve ρ_{hv} minima heights to achieve a better matching of the KBBX and NOAA snow-level radar retrievals. For the general range of precipitation SL heights during the observational period (i.e., 0.6–2.5 km MSL), the KBBX radar beam tilts, which provide observations closely representing ML regions above the snow-level radar OVL site, vary approximately from 3.1° to 10° . Figure 3 schematically shows the KBBX beam tilt measurements that were actually used for scanning radar–based ρ_{hv} minima height retrievals for different SL heights. The use of different tilt KBBX radar retrievals for different SL heights assures the best possible matching of WSR-88D and snow-level radar estimates.

b. Estimations of SL heights from operational NEXRAD level-III products

The WSR-88D melting-layer products, which are publicly available, are produced from operational radar measurements using a technique first described by Giangrande et al. (2008). This technique uses radial smoothed ρ_{hv} , Z_e , and Z_{DR} measurements at the radar beam tilt angles in the interval from 4° to 10° . At each azimuthal direction, all data from this tilt angle interval are checked to determine if they are from the ML echoes (i.e., within the predetermined intervals of radar variables expected from melting snow

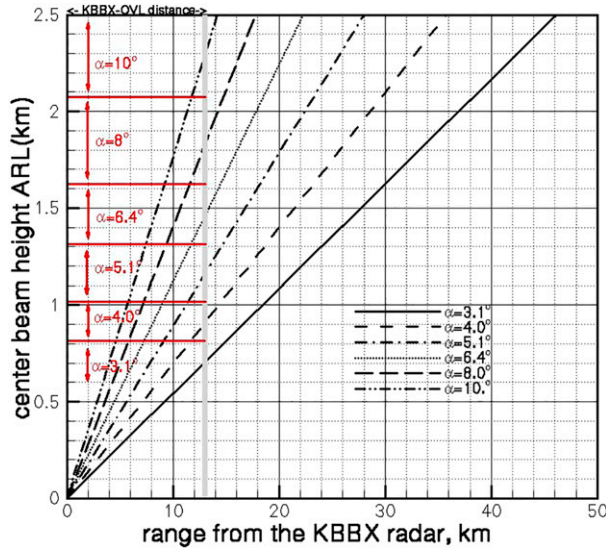


FIG. 3. KBBX beam center heights above the radar level (ARL) as the function of radar range (black lines). Arrows and tilt angles α (red) show the actual tilts that were used for KBBX ρ_{hv} minima height retrievals for subsequent intercomparisons with the OVL SL radar results at different SL heights also shown on the y axis (e.g., 5.1° KBBX tilt measurements were used when the SL heights were between about 1.02 and 1.31 km). Note that the actual KBBX tilts of 3.1° , 4.0° , 5.1° , 6.4° , 8.0° , and 10° shown in this figure are part of the volume coverage pattern 12 (VCP-12) typically used by the KBBX radar when observing precipitation.

particles). When the total count of the identified ML data points exceeds some threshold value (e.g., ~ 1500), the ML top and bottom boundaries are determined as the 80th and 20th percentile heights of ML points. In generating the ML level-III product, the azimuthal dependence of ML boundaries is smoothed using 21° running-window averaging. The operational radar ML boundaries detection procedure was subsequently further enhanced using climatological data and external information on numerical weather model output that provides the height interval where ML signatures are sought (Krause et al. 2013; Schuur et al. 2014).

The lowest WSR-88D tilt measurements are not used for ML boundaries designations, because of stronger beam broadening effects at low radar beam elevation angles. However, since lower radar beam tilt measurements are the primary ones that are used for quantitative precipitation estimates, corrections for the vertical profiles of reflectivity through accounting for ML effects are important for better precipitation retrievals. Because of the importance of these corrections, the ML boundaries that are determined for higher radar beam tilts as described above are then recalculated using the spherical Earth and mean

refraction assumptions (e.g., Doviak and Zrnić 1993, section 2.2.3) for the ML characteristics expected to be present at lower tilts. The publicly available ML data deduced from the WSR-88D measurements are stored in the NOAA National Climatic Data Center (NCDC) NEXRAD level-III products with the Advanced Weather Interactive Processing System (AWIPS) headers N0M, NAM, N1M, NBM, N2M, and N3M. These products contain the melting-layer information at low radar beam elevation angles corresponding approximately to 0.5° , 0.8° , 1.5° , 1.8° , 2.4° , and 3.1° .

For a given radar beam tilt, the information in the NEXRAD level-III ML product consists of four azimuthal arrays that contain information of estimated geographical locations where the top of the beam touches the ML bottom (latitude₁, longitude₁), the center of the beam touches the ML bottom (latitude₂, longitude₂), the center of the beam touches the ML top (latitude₃, longitude₃), and the bottom of the beam touches the ML top (latitude₄, longitude₄; Berkowitz et al. 2013; J. Krause and J. Brogden, NOAA/National Severe Storms Laboratory, 2015, personal communication). The angular resolution of the azimuthal arrays is 1° . Although the publicly available WSR-88D-based ML information is presented as geographical coordinates, it can easily be converted to the characteristic ML heights, which can be then compared to the OVL snow-level radar estimates of SL heights.

The binary NEXRAD level-III ML files corresponding to the KBBX observations were processed using the publicly available Warning Decision Support System software (Lakshmanan et al. 2007) to extract the geographical location coordinates. For given beam tilts, these coordinates (i.e., latitude_{*i*}, longitude_{*i*}; $i = 1, 2, 3$, and 4) were then converted into corresponding heights (i.e., h_i ; $i = 1, 2, 3$, and 4) using the approaches for the spherical Earth atmosphere (Doviak and Zrnić 1993, section 2.2.3). The mean value between heights h_2 and h_3 (i.e., the mean between heights where the center of the radar beam touches the ML bottom and the ML top) was then assumed to represent snow-level estimates from KBBX ML level-III products h_{L3} :

$$h_{L3} = 0.5(h_2 + h_3). \quad (2)$$

The h_{L3} estimates are generally radar azimuthal angle dependent. It should be also noted that even though the NEXRAD ML level-III products are produced for different low radar beam tilts, the same ML information collected from higher tilt measurements (i.e., from 4° to 10°) is used to derive these products.

4. A case study of 23 December 2012

A significant, mostly stratiform precipitation event was observed in the KBBX radar coverage area on 23 December 2012. The hourly mean SL estimates from the OVL snow-level radar and 2-m height air temperatures during this event are shown in Fig. 1. The event was rather deep, with cloud-top echoes exceeding at times 6 km MSL. The total integrated water vapor content, as inferred from the GPS-based measurements varied between about 20 and 24 mm, and the total rainfall accumulation at the OVL site for the period between 0900 and 2230 UTC according to the OVL site tipping-bucket type rain gauge amounted to 30.5 mm (not shown). A relatively rapid and significant increase in the snow-level heights by about 0.6 km occurred between 1800 and 1900 UTC, while the surface air temperatures changed very little during this time interval. Smaller but still significant SL height variability was also present during the first half of this precipitation event.

An example of the KBBX polarimetric WSR-88D measurements are shown in Fig. 4. This figure depicts data collected during an azimuthal angle scan at a beam elevation tilt of about 5.1° performed around 1301 UTC 23 December 2012. The melting layer is well pronounced, as observed in the reflectivity enhancement bright band and in the copolar coefficient “dark” band, but it is not seen very distinctly in differential reflectivity measurements. The reflectivity BB is wider to the east of the radar (i.e., generally toward to the OVL observational site), though its general position is quite symmetrical relative to the KBBX location. The complicated dynamics of the storm are evident from radial Doppler velocity measurements, which indicate wind velocities veering from southerly at the surface to westerly with increasing height.

KBBX radar variables observed along the beam pointing in the direction of the OVL site at the 72.1° azimuthal angle at 5.1° elevation are shown in Fig. 5. The depicted measurements are part of the azimuthal radar scan presented in Fig. 4. The data for the shortest radar ranges (<2.6 km) are generally not available. A pronounced dip of ρ_{hv} is seen near the radar range of 11 km. For the 5.1° beam tilt angle, this range approximately corresponds to the height of 1.02 km above the KBBX radar site (see Fig. 3) or $h_{\text{rtho}} \approx 1.08$ km MSL. The reflectivity BB enhancement region is significantly wider than the ρ_{hv} dip region and the largest observed Z_e values are shifted to higher altitudes (i.e., to further radar ranges) compared to the ρ_{hv} minimum height. Overall the reflectivity BB region is about 7 km wide in slant range, and it is positioned above the OVL site. Such a slant BB width approximately corresponds to a

0.6-km BB vertical thickness at the elevation angle of 5.1° . The apparent width of the reflectivity BB, however, is influenced by beam broadening effects.

Reflectivity measurements are also generally noisier compared to copolar correlation coefficient measurements, so identifying the exact positions of Z_e maxima is usually more challenging than those of ρ_{hv} minima. As evident from Fig. 5, noisiness in differential reflectivity measurements is also significant, especially in the melting-layer region, even though the maximum observed Z_{DR} values are present in this region. Differential reflectivity values in the snow region above the ML are, on average, quite low (generally less than 1 dB), indicating a presence of aggregated snowflakes. Differential reflectivity values averaging approximately 1.3 dB in the rainfall region below the ML at ranges less than 9 km (Fig. 5) are indicative of median volume raindrop diameters of about 1.8 mm (e.g., Matrosov 2010).

For the entire duration of the 23 December 2012 precipitation event, Fig. 6 shows time series of the hourly mean estimates of different parameters related to the snow-level height (i.e., h_{SL} , h_{rtho} , and h_{L3}). It can be seen that the different WSR-88D-based estimators generally reproduce the profiler-observed snow-level trends even though this event exhibited high SL variability. The robust estimates from the OVL snow-level radar profiler h_{SL} are often the highest compared to the WSR-88D estimators. The ρ_{hv} minima-based estimates h_{rtho} , which are deduced from KBBX measurements in the KBBX–OVL direction (i.e., the 72° azimuthal direction), tracks h_{SL} values rather well, including a general trend of the snow-level increase after about 1800 UTC and local maxima at around 1200 and 1430 UTC. An observed small offset between h_{SL} and h_{rtho} values is expected because of the general displacement of ρ_{hv} minima and reflectivity maxima in the ML as described previously. This offset in Fig. 6 data is nearly constant, except for the period between 1700 and 1900 UTC.

The h_{L3} estimates derived from the NEXRAD ML level-III products along the KBBX–OVL direction azimuth (the black curve in Fig. 6) also agree well with the radar values of h_{SL} , although these estimates fail to reproduce some local snow-level maxima (e.g., at around 1430 UTC). One reason for the discrepancy may be the fact that NEXRAD ML level-III products are derived from all measurements at radar beam tilt angles between 4° and 10° . It can be seen from Fig. 3 that, for an average event snow-level height of about 1.4 km, the 4° – 10° center beam tilt interval corresponds to a rather significant 8–20-km range interval from where the data are collected. This is in contrast to h_{rtho} estimates, which are obtained from the measurements at a beam tilt where the ML is observed by the KBBX radar approximately over the OVL site.

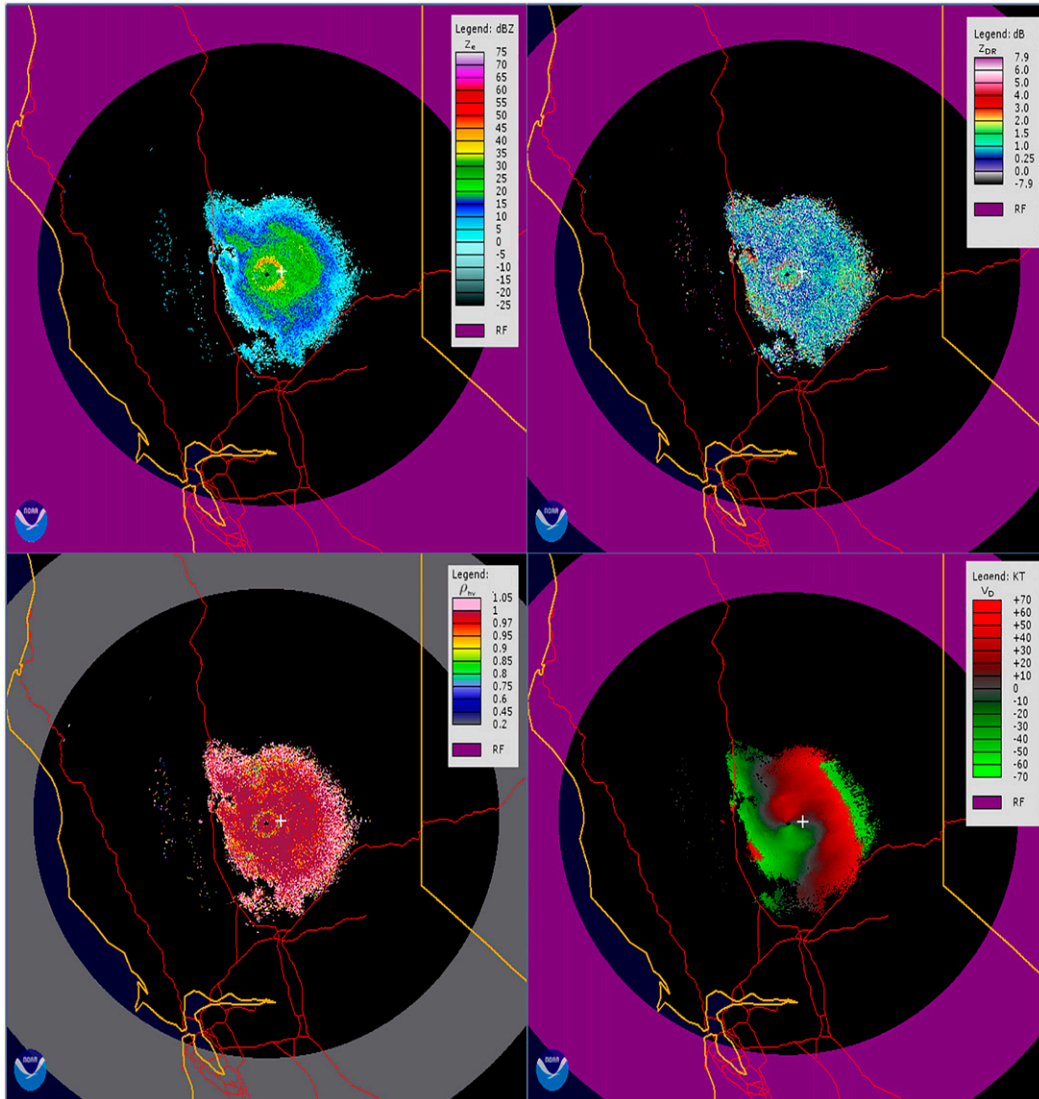


FIG. 4. Maps of the KBBX azimuthal scans at 5.1° beam elevation tilt angle at around 1303 UTC 23 Dec 2012 for (top left) Z_e , (top right) Z_{DR} , (bottom left) ρ_{hv} , and (bottom right) Doppler velocity. The coverage range (i.e., the radius of black circles) is approximately 210 km. Orange lines show coast lines and California borders, and red lines show major highways. The white plus sign shows the OVL site location.

To assess the influence of the azimuthal variability in the level-III-based SL estimates, mean and standard deviation (std dev) values of h_{L3} in the radar beam azimuth range 0° – 360° were calculated. The time series of these values are also shown in Fig. 6. It can be seen that h_{L3} azimuthal standard deviations are generally small and do not exceed 0.1 km for the precipitation event of 23 December 2012. Azimuthally averaged and 72° azimuth h_{L3} values (black and cyan curves in Fig. 6) are quite close and have very similar trends. Overall, the results presented in Fig. 6 indicate that operational polarimetric radar measurements provide reasonable estimates of SL heights, even in challenging conditions

when these heights exhibit high variability during a precipitation event.

Uncertainties in scanning radar measurements produce errors in estimating WSR-88D-based SL/ML heights. For the ranges considered in this study, a 0.1° uncertainty in radar beam pointing, for example, translates into about 20 m uncertainty in SL heights. One radar range gate (~ 250 m) error in the location of the ρ_{hv} minima along the beam results in about 28 m SL/ML height uncertainty for typical 6.4° elevation angle data. Assuming independence of these error contributions, uncertainties of around 30–40 m in SL/ML height estimates can be expected.

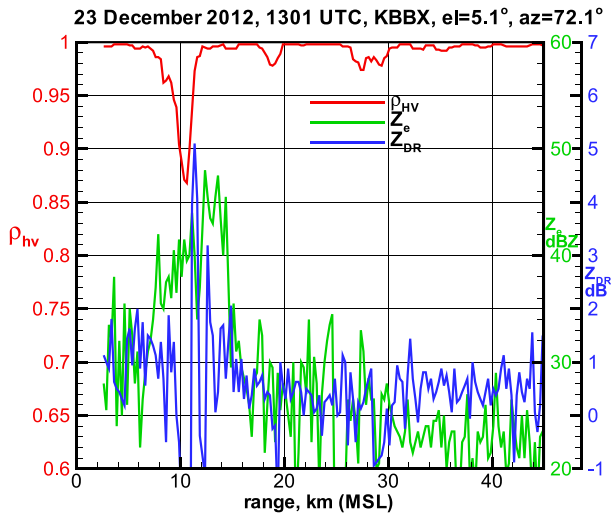


FIG. 5. KBBX measurements at 1301 UTC 23 Dec 2012 in the direction of the OVL site at the 5.1° beam elevation tilt angle.

5. Statistical intercomparisons of radar-based SL height estimates

A scatterplot of hourly mean estimates of SL heights from the OVL vertically pointing snow-level radar h_{SL} and KBBX radar ρ_{hv} minima-based estimates h_{rtho} for all the precipitation events observed during the cool season from October 2012 to March 2013 is depicted in Fig. 7. The ML/SL heights during this period varied quite significantly in a range from approximately 0.6 to more than 3 km MSL. The mean h_{SL} value was about 1.92 km MSL.

The statistical parameters (i.e., biases b , standard deviations, and correlation coefficients r) characterizing comparisons in Fig. 7 are provided in Table 1. It can be seen that there is a good correspondence between h_{SL} and h_{rtho} values. As expected, the h_{rtho} estimates are biased low relative to h_{SL} because ρ_{hv} minima are generally located below a height within the ML level, which is retrieved as the h_{SL} product from the snow-level radars (White et al. 2002, 2010) and which closely corresponds to the snow-rain transition level (Lundquist et al. 2008). The mean bias between h_{rtho} and h_{SL} is $\Delta h_b = -0.113$ km. This suggests that the height $h_{SL,rtho}$, defined as

$$h_{SL,rtho} = h_{rtho} + |\Delta h_b|, \quad (3)$$

could be considered as a good approximation to the SL heights that are inferred from the snow-level radar profiler measurements. The standard deviation of the difference between $h_{SL,rtho}$ and h_{SL} is less than 0.1 km.

Figure 8 depicts a scatterplot between snow-level radar retrievals h_{SL} and the height retrievals h_{L3} obtained using the standard NEXRAD level-III ML products from KBBX measurements. Data in this figure and in

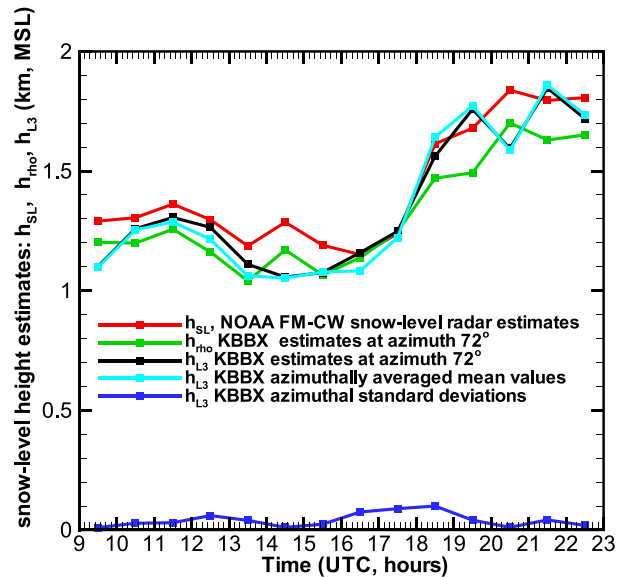


FIG. 6. Time series of different radar estimates of SL during the precipitation event observed on 23 Dec 2012.

Table 1 show that there is little statistical difference between results when h_{L3} values are derived only along the 72° azimuth in the direction from the KBBX radar site to the OVL site and when the h_{L3} values are averaged over all azimuthal directions of the KBBX

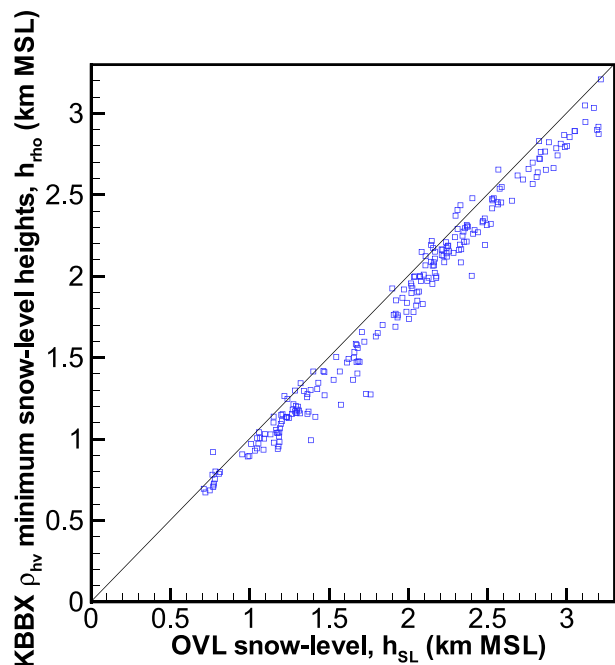


FIG. 7. A scatterplot of hourly mean OVL SL radar estimates versus KBBX ρ_{hv} minima-based estimates h_{rtho} at a 72° azimuthal direction.

TABLE 1. Bias, std dev, and correlational coefficient r values characterizing intercomparisons of different estimates of snow-level heights (h_{tho} , h_{SL} , and h_{L3}) shown in Figs. 7 and 8 for 227 hourly mean SL estimates.

	Bias (km)	Std dev (km)	Std dev after bias removal (km)	r
h_{tho} vs h_{SL} at 72° azimuth	-0.113	0.146	0.098	0.99
h_{L3} vs h_{SL} at 72° azimuth	-0.020	0.164	0.163	0.96
h_{L3} vs h_{SL} at azimuthal mean	-0.013	0.166	0.165	0.96

observations. Some larger discrepancies are seen for lower SL heights.

Figure 9 shows the standard deviation values of the h_{L3} height parameter characterizing its azimuthal variability. These values are for the most part smaller than 0.1 km, indicating a high degree of azimuthal symmetry of the KBBX level-III ML product. Some factors, which may contribute to low azimuthal variability of h_{L3} estimates, are that NEXRAD ML characteristics are derived from higher beam tilt data (thus corresponding to shorter distances as evident from Fig. 3) and are constrained by numerical weather model output, which specifies that the ML features are sought in a certain interval around a predicted 0°C isotherm height. A standard procedure of averaging the WSR-88D level-III ML products using a 21° running window in azimuth also contributes to the data azimuthal symmetry. Given the relatively low-altitude location of the OVL site, orographic effects can be relatively modest there.

These effects result in an average 0.17-km drop in the SL height between free atmosphere upwind and mountain ranges of Sierra Nevada located farther east (e.g., Minder and Kingsmill 2013).

Table 1 data indicate that the biases of the h_{L3} estimates versus h_{SL} retrievals are small, which can be explained, in part, by both quantities representing the mean heights within the ML. The h_{L3} versus h_{SL} standard deviation values, however, are higher than those for the ρ_{hv} minima-based estimates (especially for after the bias removal), reflecting the fact that the copolar correlation coefficient dips are generally narrower and are easier to identify in scanning radar data than maxima in the power measurements (i.e., Z_e and Z_{DR}), which are often wide and less well defined.

6. Discussion and conclusions

Accurate identification of snow-level (SL) heights is essential for many hydrometeorological applications since

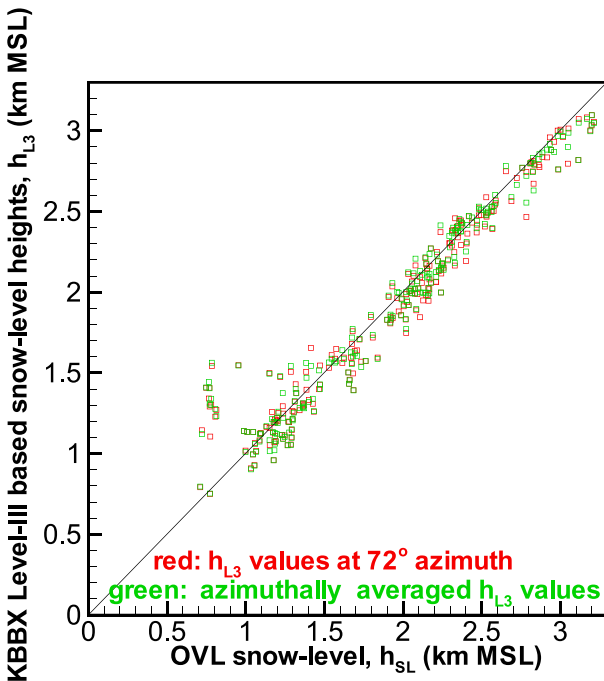


FIG. 8. A scatterplot of hourly mean OVL SL radar estimates vs KBBX level-III-based estimates h_{L3} for the period from October 2012 to March 2013.

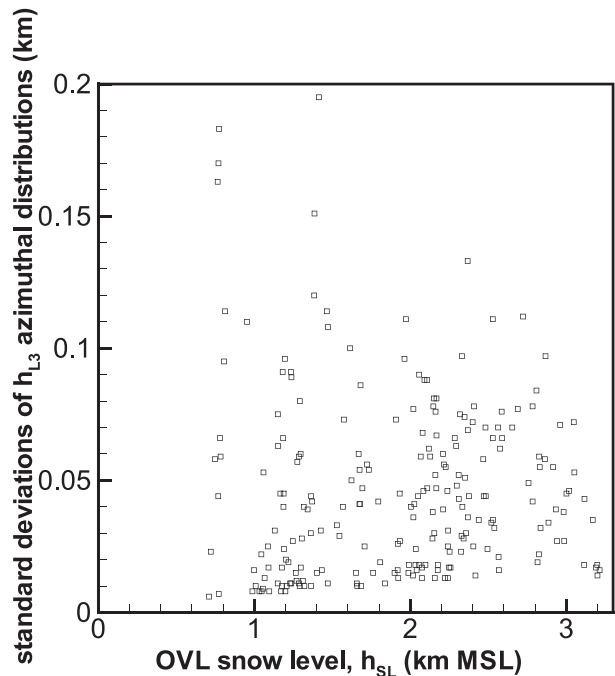


FIG. 9. A scatterplot characterizing azimuthal variability of h_{L3} estimates derived from the KBBX level-III ML products.

these heights determine the dominant precipitation phase (i.e., snow above the SL or rain below the SL). The SL height is closely related to and located under the atmospheric freezing (melting) level (FL) height, which coincides with the upper boundary of the melting layer (ML). Because of the importance of the SL information, the NOAA Hydrometeorology Testbed (<https://hmt.noaa.gov/>) operates a network of 10 dedicated high-vertical-resolution SL radar profilers near major watersheds across California as part of a twenty-first-century observing network sponsored by the California Department of Water Resources (White et al. 2013). These radars, together with several other types of NOAA/PSD profilers, provide near-real-time data on SL heights that are available to forecasters and other interested end users.

Polarimetric meteorological radar measurements allow for inferring information on ML boundaries with relatively high confidence. The recent polarimetric upgrade of the NEXRAD operational weather radar network provides an opportunity to obtain operational SL information over the areas in the vicinity of WSR-88D sites. This study evaluated the use of the existing NEXRAD level-III ML products and potential products derivable from the level-II products for retrieving the SL heights. This evaluation was performed by the intercomparisons of SL estimates from the KBBX WSR-88D measurements and robust SL retrievals h_{SL} from a nearby (~ 13 km away from the KBBX site) high-vertical-resolution FM-CW snow-level radar during the cool season precipitation period (from October 2012 to March 2013) near Oroville, California. The SL heights during the observational period varied in the approximate range of 0.6–3.2 km MSL.

The height h_{L3} , derived from the level-III ML products as the mean altitude between heights where the WSR-88D beam center touches the ML top and the ML bottom, was found to provide nearly unbiased estimates of h_{SL} with standard deviations of around 0.165 km. There was very little difference whether azimuthally averaged h_{L3} values or those obtained in the KBBX–OVL direction were used, which likely can be explained, in part, by heavy azimuthal averaging of the NEXRAD data in the level-III ML products, constraints from the numerical weather model outputs, and the fact that relatively high radar beam elevation tilts in the interval from 4° to 10° are used to derive the ML information. Because of the use of this tilt angle interval, h_{L3} estimates are characteristic of the closer WSR-88D ranges. For example, as can be seen from Fig. 3, for a mean SL height of about 1.9 km, the longest range at which level-III ML information is collected at the 4° beam tilt corresponds to about 27 km.

Retrieving the altitudes h_{rho} of the ML minima in values of copolar correlation coefficients between

horizontally and vertically polarized radar signals ρ_{hv} also provided a way for estimating SL heights. While KBBX-based h_{rho} estimates were generally biased low with respect to the snow-level radar retrievals h_{SL} by 0.113 km, the standard deviation between h_{rho} and h_{SL} was smaller and the corresponding correlation was higher compared to the h_{L3} – h_{SL} pair. After subtracting the bias, which is due to a general average altitude difference between ρ_{hv} minima and reflectivity maxima in the ML, the ρ_{hv} -based estimates $h_{SL,rho}$ were on average a better proxy to the SL height than h_{L3} . The advantage of the h_{L3} estimates, however, is that they can be relatively easily obtained from the publically available NEXRAD level-III ML products, while retrieving positions of h_{rho} ML minima from the level-II product requires applying specific algorithms not currently available in the NEXRAD level-III product suite.

Overall, the intercomparisons conducted in this study indicate that data from operational polarimetric radar measurements can provide reliable estimates of snow levels at least for close radar ranges (~ 13 – 15 km). These estimates are in good agreement with retrievals from high-spatial-resolution, vertically pointing radar profilers dedicated to SL measurements. Measurements from NEXRAD can therefore provide valuable SL information in the vicinity of WSR-88D locations, which lack dedicated SL measurements from radar profilers. Estimates of SL heights using operational radar measurements at longer distances are more challenging, in part, because of beam WSR-88D beam broadening effects. Evaluating quality of such distances requires a separate study.

Acknowledgments. This study was funded by the NOAA Physical Sciences Division in support of NOAA Hydrometeorology Testbed research under the project P8R2WCWP01.

REFERENCES

- Berkowitz, D. S., J. A. Schultz, S. Vasiloff, K. L. Elmore, C. D. Payne, and J. B. Boettcher, 2013: Status of dual pol QPE in the WSR-88D network. *27th Conf. on Hydrology*, Austin, TX, Amer. Meteor. Soc., 2.2. [Available online at <https://ams.confex.com/ams/93Annual/webprogram/Paper221525.html>.]
- Boodoo, S., D. Hudak, N. Donaldson, and M. Leduc, 2010: Application of dual-polarization radar melting-layer detection algorithm. *J. Appl. Meteor. Climatol.*, **49**, 1779–1793, doi:10.1175/2010JAMC2421.1.
- Brandes, E. A., and K. Ikeda, 2004: Freezing level estimations with polarimetric radar. *J. Appl. Meteor.*, **43**, 1541–1553, doi:10.1175/JAM2155.1.
- Bringi, V. N., and V. Chandrasekar, 2001: *Polarimetric Doppler Weather Radar*. Cambridge University Press, 636 pp.

- Doviak, R. J., and D. Zrnić, 1993: *Doppler Radar and Weather Observations*. Academic Press, 562 pp.
- Giangrande, S. E., J. M. Krause, and A. V. Ryzhkov, 2008: Automatic designation of the melting layer with a polarimetric prototype of the WSR-88D radar. *J. Appl. Meteor. Climatol.*, **47**, 1354–1364, doi:10.1175/2007JAMC1634.1.
- Keränen, R., L. C. Alku, and J. Selzler, 2015: Estimation of melting layer altitudes from dual-polarization weather radar observations. *37th Conf. on Radar Meteorology*, Norman, OK, Amer. Meteor. Soc., 1.88. [Available online at <https://ams.confex.com/ams/37RADAR/webprogram/Paper275961.html>.]
- Krause, J., V. Lakshmanan, and A. Ryzhkov, 2013: Improving detection of the melting layer using dual-polarization radar, NWP model data, and object identification techniques. *36th Conf. on Radar Meteorology*, Breckenridge, CO, Amer. Meteor. Soc., 262. [Available online at <https://ams.confex.com/ams/36Radar/webprogram/Paper228651.html>.]
- Lakshmanan, V., T. Smith, G. J. Stumpf, and K. Hondl, 2007: The warning decision support system–integrated information. *Wea. Forecasting*, **22**, 596–612, doi:10.1175/WAF1009.1.
- Lundquist, J. D., P. J. Neiman, B. Martner, A. B. White, D. J. Gottas, and F. M. Ralph, 2008: Rain versus snow in the Sierra Nevada, California: Comparing Doppler profiling radar and surface observations of melting level. *J. Hydrometeor.*, **9**, 194–211, doi:10.1175/2007JHM853.1.
- Matrosov, S. Y., 2008: Assessment of radar signal attenuation caused by the melting hydrometeor layer. *IEEE Trans. Geosci. Remote Sens.*, **46**, 1039–1047, doi:10.1109/TGRS.2008.915757.
- , 2010: Evaluating polarimetric X-band radar rainfall estimators during HMT. *J. Atmos. Oceanic Technol.*, **27**, 122–134, doi:10.1175/2009JTECHA1318.1.
- , K. A. Clark, and D. E. Kingsmill, 2007: A polarimetric radar approach to identify rain, melting-layer, and snow regions for applying corrections to vertical profiles of reflectivity. *J. Appl. Meteor. Climatol.*, **46**, 154–166, doi:10.1175/JAM2508.1.
- Minder, J. R., and D. E. Kingsmill, 2013: Mesoscale variations of the atmospheric snow line over northern Sierra Nevada: Multiyear statistics, case study, and mechanics. *J. Atmos. Sci.*, **70**, 916–938, doi:10.1175/JAS-D-12-0194.1.
- Schuur, T. J., A. V. Ryzhkov, and J. Krause, 2014: A new melting layer detection algorithm that combines polarimetric radar-based detection with thermodynamic output from numerical models. *Eighth European Conf. on Radar in Meteorology and Hydrology*, Garmisch-Partenkirchen, Germany, DWD-DLR, P05. [Available online at http://www.pa.op.dlr.de/erad2014/programme/ExtendedAbstracts/135_Schuur.pdf.]
- White, A. B., D. J. Gottas, E. T. Strem, F. M. Ralph, and P. J. Neiman, 2002: An automated brightband height detection algorithm for use with Doppler radar spectral moments. *J. Atmos. Oceanic Technol.*, **19**, 687–697, doi:10.1175/1520-0426(2002)019<0687:AABHDA>2.0.CO;2.
- , —, A. F. Henkel, P. J. Neiman, F. M. Ralph, and S. I. Gutman, 2010: Developing a performance measure for snow-level forecasts. *J. Hydrometeor.*, **11**, 739–753, doi:10.1175/2009JHM1181.1.
- , and Coauthors, 2013: A twenty-first-century California observing network for monitoring extreme weather events. *J. Atmos. Oceanic Technol.*, **30**, 1585–1603, doi:10.1175/JTECH-D-12-00217.1.
- Wolfensberger, D., D. Scipion, and A. Berne, 2016: Detection and characterization of the melting layer based on polarimetric radar scans. *Quart. J. Roy. Meteor. Soc.*, **142**, 108–124, doi:10.1002/qj.2672.